

**Structural Strength Performance of Carbon Fiber Reinforced Polymer on High
Strength Concrete Beam**

By

MUHAMMAD AZHAR BIN IBRAHIM

FINAL YEAR PROJECT REPORT

**Submitted to the Civil Engineering Programme
in Partial Fulfillment of the Requirements
for the Degree
Bachelor of Engineering (Hons)
(Civil Engineering)**

**Universiti Teknologi Petronas
Bandar Seri Iskandar
31750 Tronoh
Perak Darul Ridzuan**

© Copyright 2008

by

Muhammad Azhar bin Ibrahim, 2008

CERTIFICATION OF APPROVAL

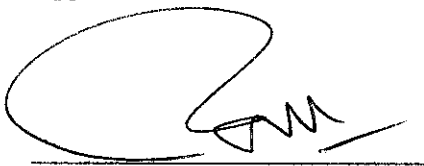
**Structural Strength Performance of Carbon Fiber Reinforced Polymer on High
Strength Concrete Beam**

by

Muhammad Azhar bin Ibrahim

A project dissertation submitted to the
Civil Engineering Programme
Universiti Teknologi PETRONAS
in partial fulfilment of the requirement for the
Bachelor of Engineering (Hons)
(Civil Engineering)

Approved:



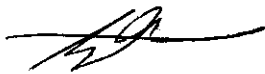
Dr. Nasir Shafiq
Project Supervisor

**UNIVERSITI TEKNOLOGI PETRONAS
TRONOH, PERAK**

January 2008

CERTIFICATION OF ORIGINALITY

This is to certify that I am responsible for the work submitted in this project, that the original work is my own except as specified in the references and acknowledgements, and that the original work contained herein have not been undertaken or done by unspecified sources or persons.



Muhammad Azhar bin Ibrahim

ABSTRACT

The existing public infrastructures of Malaysia has suffered from decades of neglect and overuse, leading to the accelerated deterioration of bridges, building, transportation systems, and resulting in a situation that approaching a infrastructure crisis. This paper investigates the flexural behavior of Carbon Fiber Reinforced Polymer (CFRP) plates on high strength concrete beams. Eight concrete beam specimens with dimensions of 150 mm width, 200 mm height and 2150 mm length to give a clear span length of 2000 mm were manufactured and tested. These eight beams were grouped by four CB-series beams which were made without fly ash replacement and four CF-series beams which were made with 30% fly ash replacement. Six of the reinforced concrete beams were externally strengthened by pasting CFRP plates at the soffit of the beam, three different lengths, 1333 mm, 1667 mm and 2000 mm which represent 66.7%, 83% and 100% respectively of the total beam span. The optimum length of the CFRP plate was then established for structural strengthening in terms of load carrying capacity, ductility and economical factor. The results have shown that 1667 mm which is 83% of the span length is the optimum length of the CFRP plate that achieved the highest strength; beyond this length, the increase in the strength was negligible considering the economical factor. The behavior of reinforced concrete beams made of 30% fly ash replacement and those made of normal concrete was similar at first crack and ultimate loads when externally strengthened with CFRP plates.

ACKNOWLEDGEMENTS

The author wishes to take the opportunity to express his utmost gratitude to the individual that have taken the time and effort to assist the author in completing the project. Without the cooperation of these individuals, no doubt the author would have faced some minor complications through out the course.

First and foremost the author's utmost gratitude goes to the author's supervisor, Dr. Nasir Shafiq and author's mentor, Asma Abd Elhameed Hussein for their guidance, advice and patience. To the Final Year Project Coordinator, Miss Niraku Rosmawati and Mr. Kalaikumar for all the initial information required to begin the project and for all the lecture series organized.

To the entire technicians in Civil Engineering Department, thank you for assisting the author in completing the project.

To all individuals that has helped the author in any way, the author thank you all.

TABLE OF CONTENTS

LIST OF TABLES	vii
LIST OF FIGURES.....	viii
LIST OF ABBREVIATIONS	ix
CHAPTER 1 INTRODUCTION	1
1.1 Background	1
1.2 Problem Statement	1
1.3 Objectives.....	2
1.4 Scope of Study.....	2
CHAPTER 2 LITERATURE REVIEW	3
2.1 Introduction	3
2.2 Flexural strengthening using CFRP composites	3
2.3 Disadvantages of external strengthening using steel plates	5
CHAPTER 3 METHODOLOGY	7
3.1 Mixing of Concrete and Formwork Preparation	7
3.1.1 Concrete Mixing Procedure	8
3.2 Materials.....	9
3.2.1 Concrete.....	9
3.2.1.1 Cement.....	9
3.2.1.2 Pulverized Fuel Ash (PFA)	9
3.2.1.3 Aggregates.....	10
3.2.1.4 Superplasticizer	12
3.2.1.5 Water	12
3.2.2 Reinforcing Steel	13
3.2.3 Carbon Fibre Reinforced Polymer.....	13
3.2.3.1 Introduction	13
3.2.3.2 CFRP strips.....	13
3.2.3.3 Adhesive	14
3.3 Strengthened Beams.....	14
3.3.1 Design of Beams.....	14
3.3.2 CFRP Installation.....	15
3.3.2.1 Concrete Surface Preparation.....	15

3.3.2.2 CFRP Bonding	16
3.3.3 Instrumentation	21
3.4 Testing Procedure.....	21
CHAPTER 4 RESULT AND DISCUSSION	22
4.1 Modes of Failure, Crack Pattern and Failure Load	22
4.2 Effects of CFRP length.....	25
4.3 Load – Deflection Behaviour	26
4.4 CB – Series.....	27
4.5 CF – Series	28
4.6 Ductility.....	29
CHAPTER 5 CONCLUSION.....	31
REFERENCES.....	32
APPENDIX 3.1	34
APPENDIX 3.2	36
APPENDIX 3.3	38
APPENDIX 3.4.....	40
APPENDIX 4.1	43

LIST OF FIGURES

Figure 1 : Beam Dimensions and Reinforcement Details.....	15
Figure 2 : External Reinforcement for CB2 and CF2	17
Figure 3 : Area Covered by CFRP Plate for 67% of the length.....	18
Figure 4 : External Reinforcement for CB3 and CB4.....	19
Figure 5 : Area Covered by CFRP Plate for 83% of the length.....	19
Figure 6 : External Reinforcement for CB4 and CF4	20
Figure 7 : Area Covered by CFRP plate for 100% length	20
Figure 8 : Beam Instrumentation.....	21
Figure 9 : Test Setup	21
Figure 10 : Ultimate Failure Loads for The Tested Beams.....	22
Figure 11 : Schematic Drawing and Picture of CB1 Crack Patterns	23
Figure 12 : Schematic Drawing and Picture of CF1 Crack Patterns.....	23
Figure 13 : Schematic Drawing and Picture of CB2 Crack Patterns	23
Figure 14 : Schematic Drawing and Picture of CF2 Crack Patterns.....	24
Figure 15 : Schematic Drawing and Picture of CB3 Crack Patterns	24
Figure 16 : Schematic Drawing and Picture of CF3 Crack Patterns.....	24
Figure 17 : Schematic Drawing and Picture of CB4 Crack Patterns	25
Figure 18 : Schematic Drawing and Picture of CF4 Crack Patterns.....	25
Figure 19 : Load – Deflection Relationship For The CB- Series.....	26
Figure 20 : Load – Deflection Relationship For The CF- Series	27
Figure 21 : Ultimate Mid – Span Deflection For All Tested Beams	27

LIST OF ABBREVIATIONS

CFRP	Carbon Fiber Reinforced Polymer
MPa	Mega Pascal
p_{max}	maximum reinforcement ratio
mm	Milimeter
kg	Kilogram
m	Meter
A_{frp}	area of Fiber Reinforced Polymer shear reinforcement
A_g	gross cross-sectional area of the column
A_{st}	area of longitudinal tensile or vertical reinforcing steel
A_s	area of compressive flexural reinforcing steel
A_v	area of the transverse steel shear reinforcement
C_c	concrete compressive flexural stress resultant
C_s	compression steel flexural stress resultant
c	neutral axis depth
d	effective depth of cross-section
E_{frp}	Fiber Reinforced Polymer reinforcement modulus of elasticity
E_s	steel reinforcement modulus of elasticity
f_c	concrete stress (less than ultimate)
f'_c	concrete compressive strength
f_{frp}	stress in Fiber Reinforced Polymer reinforcement (less than ultimate)
f_{frpu}	ultimate strength of Fiber Reinforced Polymer reinforcement
f_{lfrp}	lateral confining pressure exerted by the Fiber Reinforced Polymer at ultimate
f_s	stress in tensile flexural steel reinforcement (less than yield)
f'_s	stress in compressive flexural steel reinforcement (less than yield)
f_y	yield stress of steel reinforcement
L	span of a beam
L_e	effective length of a column
M_r	moment resistance of a cross-section
P_f	factored axial load on a column
P_D	axial dead load requirement for a column
P_L	axial live load requirement for a column

P_{max}	factored axial load resistance for an Fiber Reinforced Polymer-confined reinforced concrete column
s	spacing of the transverse steel shear reinforcement
T_{frp}	Fiber Reinforced Polymer tensile flexural stress resultant
T_s	reinforcing steel tensile flexural stress resultant
t_{frp}	total thickness of Fiber Reinforced Polymer reinforcement
V_c	factored shear resistance attributed to the concrete
V_{frp}	factored shear resistance attributed to the Fiber Reinforced Polymer
V_r	factored shear resistance
V_s	factored shear resistance attributed to the steel reinforcement
w_{frp}	width of Fiber Reinforced Polymer shear reinforcement measured perpendicular to fibres
α	reduction coefficient for the effective strain in the Fiber Reinforced Polymer
α_1	ratio of average stress in rectangular compression block to the specified concrete compressive strength
α_{pc}	performance coefficient for Fiber Reinforced Polymer confined concrete
β	angle between inclined Fiber Reinforced Polymer stirrups and the longitudinal axis of the member
β_1	ratio of depth of rectangular compression block to depth of the neutral axis
ϵ_c	strain in concrete
ϵ_{cu}	ultimate compressive strain of concrete
ϵ_{frp}	strain in Fiber Reinforced Polymer reinforcement
ϵ_{frpe}	effective strain of Fiber Reinforced Polymer reinforcement
ϵ_{frpu}	ultimate strain of Fiber Reinforced Polymer reinforcement
ϵ_s	total strain in tension steel reinforcement
ϵ'_s	total strain in compression steel reinforcement
ϵ_y	yield strain of steel
ϕ_c	resistance factor for concrete
ϕ_{frp}	resistance factor for Fiber Reinforced Polymer
ϕ_s	resistance factor for steel reinforcing bars
λ_1	coefficient for the effective strain in the Fiber Reinforced Polymer
λ_2	coefficient for the effective strain in the Fiber Reinforced Polymer
ρ_{frp}	Fiber Reinforced Polymer shear reinforcement ratio

CHAPTER 1

INTRODUCTION

1.1 Background

In the last ten to fifteen years, Carbon Fiber Reinforced Polymer (CFRP) materials have emerged as promising alternative repair the members of reinforced concrete structures, and they are rapidly becoming materials of choice for strengthening and rehabilitation of concrete infrastructure. CFRP plates or sheets can be bonded to the exterior of concrete structures using high-strength adhesives to provide tensile or confining reinforcement which supplements that provided by internal reinforcing steel. CFRP materials are non-corrosive and nonmagnetic, and can thus be used to eliminate the corrosion problems invariably encountered with conventional repair materials such as externally-bonded steel plates. In addition, CFRPs are extremely light, strong, highly versatile, and comparatively easy to install, making them ideal materials for the repair and strengthening of concrete structures.

1.2 Problem Statement

Beams are critical part of buildings. Their constituent materials have a limited strength. Whenever forces applied are larger than their capacity due to overuse or deterioration, severe damaged or failure will occur. Reconstruction of the structure will be not economical. Thus, rehabilitation schemes by using CFRP material and the effect of this material to concrete beams must be studied. There was no study on the behaviour of fly ash concretes beams when strengthened with CFRP composites. A few research been done to investigate the effective length of CFRP plate to be used for flexural strengthening of reinforced concrete beams and achieve the highest load carrying capacity and the full span length was adopted which is not economical.

1.3 Objectives

- To investigate the flexural behavior, in terms of ultimate load capacity and ductility ratio, of reinforced concrete beams strengthened with externally bonded carbon fiber reinforced polymer (CFRP) strips having different lengths in order to determine the optimum length of CFRP plate.
- To compare the flexural behavior of reinforced concrete beams made of normal and fly ash concrete strengthened with CFRP plates.

1.4 Scope of Study

- Cast eight 150*200*2000 mm reinforced concrete beams and calculate flexural/bending capacity and shear capacity of the casted beams.
- Flexural test on 150*200*2000 mm reinforced concrete beams strengthened with CFRP strips.
- Sieve analysis for the aggregates used to manufacture the beams.
- Analyze the optimum CFRP length for the reinforced concrete beam and the effect of the fly ash.

CHAPTER 2

LITERATURE REVIEW

2.1 Introduction

It is common where problems arise when existing concrete structures or some of their components found to be inadequate and in need of repair and/or strengthening. One of the primary factors leading to the unsatisfactory state of the structure is corrosion of the reinforcing steel inside the concrete. A common feature that causes deterioration is that there is a reduction of the alkalinity of the concrete, which allows oxidation of the reinforcing steel to take place. This oxidation process leads to cracking of the concrete and possible spalling of the cover to the reinforcement [Waleed A. Thanoon et al. (2005)]. The following chapter discusses the literature review, this review is important as a first step to start this project and it will definitely help in setting up the experiments. This review focus on methods of strengthening, especially steel plate bonding and FRP composite bonding, effects of CFRP plates as strengthening material, and the mode of failures.

2.2 Flexural strengthening using CFRP composites

M. R. Esfahani et al., (2007) performed an experiment on reinforced concrete beams externally strengthened with CFRP sheets with different reinforcement ratios. Twelve reinforced concrete beams each of 150 mm width, 200 mm height and 2000 mm length were manufactured with concrete compressive strength of 25 MPa and cement content of 350kg/m³ and tested in four – point bending. They obtained that with large reinforcement ratio close to the maximum reinforcement ratio, ρ_{max} . failure of the strengthened beams occur in either interfacial debonding induced by flexural crack, or interfacial debonding induced by flexural – shear crack with adequate ductility.

Omrane Benjeddou et al., (2007) tested eight reinforced concrete beams while investigating the behaviour of damaged reinforced concrete beams repaired by bonding of carbon fibre reinforced plastic laminates. All test beams were 120 mm wide, 150 mm high and 2000 mm long. The main parameters investigated were damage degree, CFRP laminate width and concrete strength class. The concrete compressive strengths were 21 MPa and 38 MPa and normal concrete was used. The CFRP laminate width was varied from 50 to 100 mm and the length of all laminates used was 1700 mm. An increase in the load capacity for the beam that was directly strengthened (not damaged) about 87% over the control beam was obtained. Two failure modes were observed for strengthened and repaired beams, namely, peeling off and interfacial debonding. The former was observed for all reinforced beams with the laminate width of 100 mm while the latter was observed for all reinforced beams with the laminate width of 50 mm. an increase in load carrying capacity from 40 – 87% was obtained.

A test performed by H. Toutanji et al., (2006) in which eight reinforced concrete beams were tested and analyzed: one control beam and seven beams reinforced with three to six layers of CFRP sheets bonded by inorganic epoxy. The test results showed that increasing the number of layers of CFRP sheets increase the load – carrying capacity while reducing the ductility of the strengthened reinforced concrete beams. For three and four layers of reinforcement beams failed by the rupture of carbon fibre sheet, but for six layers of FRP reinforcement beams failed by FRP delamination.

Ali Chahrour and Khaled Soudki, (2005) tested six reinforced concrete beams to investigate the flexural response of reinforced concrete beams strengthened with CFRP strips each beam was 150 mm wide, 250 mm deep and 2400 mm long, the compressive strength of the concrete was 39 MPa. The observed mode of failure for the strengthened beams was the flexural shear crack – induced interfacial debonding type. Externally bonded CFRP strips significantly increased the ultimate capacity of reinforced concrete beams (an increase up to 45% was obtained) while reducing the ductility.

A paper presented by M. A. Shahawy et al., (1996) presents the test results of four reinforced rectangular concrete beams externally strengthened in flexure with bonded CFRP laminates. All beams were 203 mm wide, 305 mm high and 2744 mm long.

The concrete used in this investigation had compressive strength of about 29 and 41 MPa. The CFRP laminate had 0.171 mm thickness and approximately 300 mm width the beams were strengthened over the full span length. The main variables were the number of CFRP layers. It is shown that bending capacity can be increased considerably by bonding CFRP laminates to the tension side of beams, an increase of 13, 66 and 92% for the beams strengthened with 1, 2 and 3 layers of CFRP laminates respectively over the control beam was obtained . A reduction in deflection could also be achieved.

Tom Norris et al., (1997) performed an experiment to study the effect of precracking of beams before strengthening with carbon fibre sheets. The importance of fibre direction was also examined. Nineteen beams were tested under four – point bending. They found that there was no difference in behaviour between the precracked beams and non – precracked ones at the ultimate level, the most significant differences were due to the fibre orientations; when CFRP fibres were placed perpendicular to cracks in a concrete test beam, a large increase in stiffness and flexural strength was observed and brittle failure occurred due to concrete rupture. When the CFRP fibres were placed obliquely to the cracks in the beam, a smaller increase in strength and stiffness was observed, however the mode of failure was more ductile.

2.3 Disadvantages of external strengthening using steel plates

The in situ rehabilitation or upgrading of RC beams using bonded steel plates has been proven in the field to control flexural deformations and crack widths, and to increase the load – carrying capacity of the member under service load for ultimate conditions. It is recognized to be an effective, convenient and economic method of improving structural performance. However, although the technique has been shown to be successful in practice, it also has disadvantages. Since the plates are not protected by the concrete in the same way as the internal reinforcement, the possibility of corrosion exists which could adversely affect the bond strength, leading to failure of the strengthening system. Uncertainty remains regarding the durability and the effects of corrosion. To minimize the possibility of corrosion, all chloride – contaminated concrete should be removed prior to bonding and the plates must be subjected to careful surface preparation, storage integrity of the primer must be periodically checked, introducing a further maintenance task to the structure. The

plates are generally prepared by grit blasting, which unless a minimum thickness of typically 6 mm is imposed can cause distortion. Steel plates are difficult to shape in order to fit complex profiles. In addition, the weight of the plates makes them difficult to transport and handle on site, particularly in areas of limited access, and can cause the dead weight of the structure to be increased significantly after installation. Elaborate and expensive falsework is required to maintain the steelwork in position during bonding. The plates are required to be delivered to site within flatness tolerances to prevent stresses being introduced normal to the bondline during cure. The weight of the plate and this flatness requirement generally restricts the maximum plate length to between 6 – 8 m. since the spans requiring strengthening are often greater than this length, joints are required. Welding cannot be used in these cases since this would destroy the adhesive bond. Consequently lapped butt joints have to be formed, adding further complications to the design of the system. Studs are required to assist in supporting the steel plates during installation and under service loading conditions. This is especially true towards the ends of the plates where anchorages are required due to the high bending stiffness of the plate. The position of these studs must therefore be established prior to bonding. This process can involve a considerable amount of site work. Finally, if the plates are loaded in compression, buckling may occur, causing the plates to become detached. The process involved in strengthening with steel plates can therefore be considered as relatively time consuming and labour intensive [L C Hollaway and M B Leeming, (1999)].

CHAPTER 3

METHODOLOGY

3.1 Mixing of Concrete and Formwork Preparation

In this research a total of eight reinforced concrete beams were designed and constructed according to (BS8110) code of practice. Four beams contained 30% fly ash and the remaining four beams were made of normal concrete. Six beams were externally strengthened with CFRP plates at the soffit of the beam with different length as shown in Table 1.

Table 1 : Summary of Beam Properties

Beam ID	Beam dimensions (mm)					Concrete properties			Tension reinforcement			FRP properties				
	<i>b</i>	<i>h</i>	<i>d</i>	<i>L</i>	<i>A</i>	<i>PFA</i>	<i>f_{cu}</i>	<i>E_c</i>	<i>f_y</i>	<i>E_s</i>	<i>A_s</i>	<i>L_{frp}</i>	<i>L_{frp}</i>	<i>A_f</i>	<i>E_f</i>	<i>ε_{fu}</i>
						(%)	(MPa)	(GPa)	(MPa)	(GPa)	mm ²	mm	(%)	mm ²	(GPa)	(%)
CB1	150	200	161	2150	1000	0	66	34	460	230	402	0	0	120	150	1.4
CF1	150	200	161	2150	1000	30	69	34	460	230	402	0	0	120	150	1.4
CB2	150	200	161	2150	1000	0	66	34	460	230	402	1333	67	120	150	1.4
CF2	150	200	161	2150	1000	30	69	34	460	230	402	1333	67	120	150	1.4
CB3	150	200	161	2150	1000	0	66	34	460	230	402	1667	83	120	150	1.4
CF3	150	200	161	2150	1000	30	69	34	460	230	402	1667	83	120	150	1.4
CB4	150	200	161	2150	1000	0	66	34	460	230	402	2000	100	120	150	1.4
CF4	150	200	161	2150	1000	30	69	34	460	230	402	2000	100	120	150	1.4

3.1.1 Concrete Mixing Procedure

The following points describe the procedure used for mixing of all samples:

- Measure all the mix ingredients in the proportions and make sure that all the metal instruments and tools are moist (mixing drum, trowels, mixing trays, and rods). This to ensure that the moisture content is not drastically reduced by the properties of the metallic instruments and also to make sure that there is no standing water in mixing drum or pans.
- Place the coarse and fine aggregate into the mixing drum. Turn on the mixer and allow it to mix for 25 seconds.
- Add half of water and mix for one minute and leave it for eight minutes.
- Mix the cementitious materials (cement or/and fly ash) together in a container and place it into the mixing drum and mix for one minute.
- Pour the remaining water (with the required superplasticizer) and mix for one minute.
- Do hand mixing to ensure homogeneity.
- Lower the handle of the concrete mixer and pour the contents out into a moistened pan.

The workability and consistency of the concrete mixes were measured according to BS 1881: Part 102: 1983 using the slump cone test. The mould for the slump test is a frustum of a cone, 300 mm high. It was placed on a smooth surface with the smaller opening at the top and it was firmly held against its base during the entire operation; this was facilitated by foot – rest brazed to the mould. The mould was filled with concrete in three layers. Each layer was tamped 25 times with a standard 16 mm diameter steel rod, rounded at the end, and the top surface was struck off by means of sawing and rolling motion of the tamping rod. Immediately after filling, the cone was slightly lifted; the decrease in the height of slumped concrete was measured to the highest point.

3.2 Materials

Materials used in this research were studied separately to acquire the properties which can be important information in analyzing the behavior of the specimens.

3.2.1 Concrete

The concrete properties included ordinary Portland cement (OPC), pulverized fuel ash (PFA) as a cement replacement material, mining sand for fine aggregate, granite gravel for coarse aggregate, superplasticizer as water reducing admixture and water. A 50 MPa compressive strength was chosen to simulate tall buildings. Each element in concrete is discussed below.

3.2.1.1 Cement

A commercially available ordinary Portland cement Type 1 according to BS 12 was used for all concrete mixes and for beam construction. Chemical properties of OPC are shown in Table 2.

Table 2 : Chemical Properties of Ordinary Portland Cement

Chemical constituents	Percentage, (%)
Silicon dioxide (SiO ₂)	21.98
Aluminum dioxide (Al ₂ O ₃)	4.65
Ferric oxide (Fe ₂ O ₃)	2.27
Calcium oxide (CaO)	61.55
Magnesium oxide (MgO)	4.27
Sulfur oxide (SO ₃)	2.19
Potassium oxide (K ₂ O)	1.04
Sodium oxide (Na ₂ O)	0.11

3.2.1.2 Pulverized Fuel Ash (PFA)

The fly ash used in this study was obtained from Manjung Power Station at Lumut, Perak and is classified as low lime fly ash and ASTM Class F fly ash. Chemical composition and physical properties of fly ash are given in Table 3.

Table 3 : Chemical Composition and Physical Properties of Fly Ash

Chemical constituents	Percentage, %
Silicon dioxide (SiO ₂)	56.39
Aluminum dioxide (Al ₂ O ₃)	17.57
Ferric oxide (Fe ₂ O ₃)	9.07
Calcium oxide (CaO)	11.47
Magnesium oxide (MgO)	0.98
Sulfur oxide (SO ₃)	0.55
Sodium oxide (Na ₂ O)	1.91
Potassium oxide (K ₂ O)	1.98
Physical properties	
Specific gravity	2.37
Fineness, (m ² /kg)	243

3.2.1.3 Aggregates

Soils may be divided on basis of their dominating particle size into six arbitrary categories which are boulders, cobbles, gravel, sand, silt and clay. The size ranges of particles in each group are categorized according to the British Standard as defined in BS5930:1981. The following points describe the procedure used for sieve analysis.

- A set of sieves of each diameter prepared. Weight and record each sieves.
- Oven dry the sample overnight in an oven maintained at 105 – 110°C.
- Put the sample on top and use a mechanical shaker for sieving. Agitation in the shaker is for a minimum period of 10 minutes.
- Weight and record each sieves.

The form recommended in British Standard for presenting aggregate distribution is the particle size distribution curve shown in the Appendix 3.1 and Appendix 3.2 from the data obtained from the sieve analysis. On this standard chart, it enables to recognise instantly the grading characteristics of a soil than tabulated figures. The position of a curve on the chart indicates the finess or coarseness of the aggregates.

The steepness, flatness and general shape indicate the distribution of aggregate sizes within the soil. [Head K.H, 1993]

3.2.1.3.1 Fine Aggregate

The fine aggregate used for all the mixes are from Tronoh, Malaysia. The sieve analysis test for fine aggregate is shown in Table 4.

Table 4 : Sieve Analysis for Fine Aggregates

Sieve Size	Weight Retained (g)	% Retained	% Cumulative Weight Retained	% Total Passing
2.36 mm	110.3	11.03	11.03	88.97
2 mm	30.4	3.04	14.07	85.93
1.18 mm	118.1	11.81	25.88	74.12
0.6 mm	230.2	23.02	48.9	51.1
0.425 mm	125.2	12.52	61.42	38.58
0.3 mm	135.1	13.51	74.93	25.07
0.15 mm	180.3	18.03	92.96	7.04
0.075 mm	60.2	6.02	98.98	1.02
Pan	10.2	1.02	100	0

Total = 1000 g

And from the curve in Appendix 3.1, it can be seen that it is a well graded fine aggregate. Please refer to Appendix 3.1 for the particle size distribution curve.

3.2.1.3.2 : Coarse Aggregate

Granite gravel with a maximum particle size of 20 mm and it was obtained from Papan granite, Ipoh, Malaysia. The sieve analysis for coarse aggregate is shown in Table 5. Both fine and coarse aggregates conforming to BS 882: 1992.

Table 5 : Sieve Analysis for Coarse Aggregates

Sieve Size	Weight Retained (g)	% Retained	% Cumulative Weight Retained	% Total Passing
20 mm	77	2.82	2.82	97.18
14 mm	579	21.17	23.99	76.01
10 mm	780	28.52	52.50	47.50
5 mm	1052	38.46	90.97	9.03
3.35 mm	102	3.73	94.70	5.30
Pan	145	5.30	100.00	0.00

Total = 2735 g

From the particle size distribution curve in Appendix 3.2, it can be seen that the slope between D_{60} and D_{10} is slightly steep. Thus, the result is slightly poor sorted coarse aggregate. Please refer to Appendix 3.2 for particle size distribution curve.

This is acceptable as during the mix between the cement and aggregate (coarse and fine) all the particles are ensured to be homogeneous and interlocking between the particles ensure the bonding between the aggregate and the cement.

3.2.1.4 Superplasticizer

The superplasticizers are a category of water – reducing agents in that they are formulated from materials that allow much greater water reductions, or alternatively extreme workability of concrete in which they are incorporated. This is achieved without undesirable side effects such as excessive air entrainment or set retardation [Roger Rixom and Noel Mailvaganam, (1999)]. Commercially available, Sikament – NI, superplasticizer in the form of aqueous solution was used as water reducing admixture (WRA) for all concrete mixes. It was a naphthalene formaldehyde sulphonate superplasticizer.

3.2.1.5 Water

The tap water was used for mixing and curing of all concrete mixes and hardened concrete respectively.

3.2.2 Reinforcing Steel

The longitudinal reinforcement was high yield steel deformed bars with a diameter of 16 mm for the tensile bars with a yield strength, modulus of elasticity, ultimate strain of 460 MPa, 230 GPa and 0.002 respectively. The shear reinforcement consisted of vertical stirrups of 6 mm diameter with characteristics strength of 250 MPa.

3.2.3 Carbon Fibre Reinforced Polymer

3.2.3.1 Introduction

A composite consists of two or more materials combined to produce a product that exceed their individual properties. In particular, fibre reinforced plastics is a combination of high – strength fibres and a matrix. The fibre is the strength of the composite, and the matrix is the product that holds the fibres together and acts as a load transfer median. Common fibres used for civil engineering projects are glass, carbon and aramid. The carbon fibres are stronger and stiffer than most other fibres, more corrosion resistant, lower in density and more widely available as a raw material. The matrix supports the fibres, protects them and transfers the loads through shear stresses.

3.2.3.2 CFRP strips

The carbon fibre reinforced plastic (CFRP) strips used in this research were Sika CarboDur S1012 of 100 mm width and 1.2 mm thickness. The properties of Sika CFRP strips as described by the supplier are shown in Table 6. The design and analysis for CFRP strips are shown in Appendix 3.3.

Table 6 : Properties of Sika's CFRP System

	Tensile strength (MPa)	Elongation at break (%)	Elastic modulus (GPa)	Compressive strength (MPa)	Adhesive strength on concrete (MPa)	Adhesive strength on steel (MPa)
Sika CFRP strip ^a	>2400	1.4	150	–	–	–
SikaDur – 30 adhesive	–	–	12.8	> 100	> 2	> 25

3.2.3.3 Adhesive

The strips were bonded to the soffit of the beams using epoxy SikaDur – 30. The epoxy resin used in this research consists of two components; part A is in white colour; part B is in dark grey. The mix ratio of part A and part B is three to one by quantity ratio. The mixture of the two is in light grey. The properties of the Sikadur – 30 adhesive are shown in Table 6 as well.

3.3 Strengthened Beams

The strengthened beams were designed to examine their flexural strength. Overall, eight reinforced concrete beams were constructed; six of which were strengthened with CFRP strips. The others were tested without CFRP and served as the control beams. This section will describe the philosophy of the design, the CFRP application and instrumentation.

3.3.1 Design of Beams

The beams were designed to study the flexural response of a strengthened slab beam in a high building. All beams were 150 mm in width, 200 mm in height and 2150 mm in length to give a clear span length of 2000 mm. The concrete cover for steel is 39 mm giving an effective depth of 161 mm. Two 16 mm bar diameter were used as a

tensile reinforcement. Please refer to Appendix 3.4 for the beam design and analysis. A critical part of the design was ensuring the beams failed due to flexure and not shear. To accomplish this, the shear stirrups were closely spaced; stirrups with 6 mm diameter were used for shear strengthening and spaced at 100 centre to centre. The design was based on BS 8110: PART 1: 1997. A sketch for beam dimensions with longitudinal reinforcement and stirrup spacing is shown in Figure 3.1. The specimens were moulded in plywood boxes, and prior to casting, the mold walls were painted with lubricating oil to prevent adhesion with the cured concrete. The concrete was vibrated and kept in a moist environment by using plastic sheets. Specimens were demoulded after twenty four hours, and sprayed with water every day.

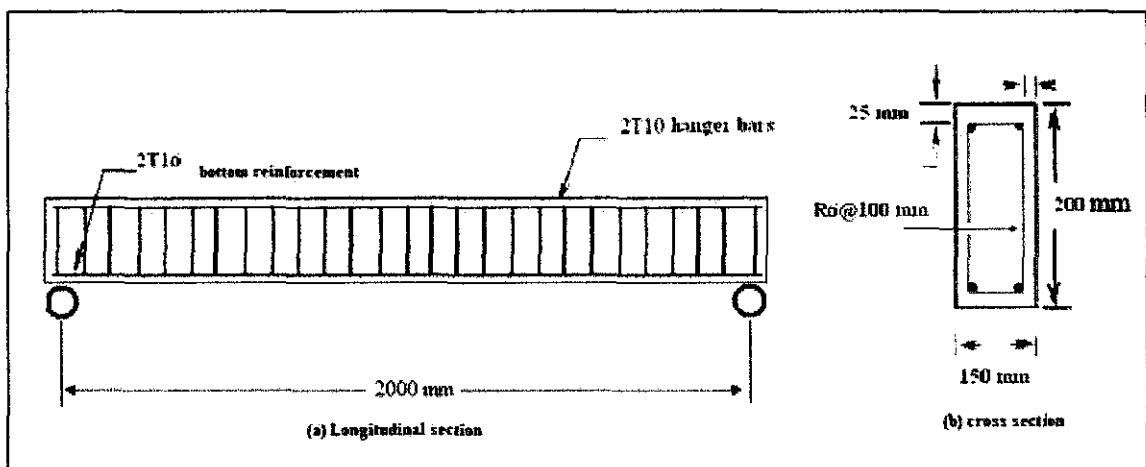


Figure 1 : Beam Dimensions and Reinforcement Details

3.3.2 CFRP Installation

The most important factor in creating a composite system with reinforced concrete beam and CFRP is assuring the bond between the materials is adequate. Preparation of the concrete surface and the application of the CFRP are discussed in the following section.

3.3.2.1 Concrete Surface Preparation

It was necessary to have a level concrete surface to serve as a bonding plain for the CFRP. Also, the surface should be independent from all unwanted particles such as dust or grease. To achieve these, an electrical hand held steel grinder was used to remove the weak surface layer on the tension side of the beam. Nonelectrical manual

steel brush was also used to help for the same purpose mentioned above. The preparation was complete by blowing the specimen with compressed water to remove any excess particles.

3.3.2.2 CFRP Bonding

To investigate the effective length of CFRP plate for optimum strengthening, three different lengths were chosen. For each studied length two beams were constructed. The procedure of bonding the CFRP to the beams is discussed below:

- The CFRP plates were cut to the required length.
- The CFRP plates were cleaned with acetone, this process was repeated until the washcloth was no longer blackened.
- The reinforced concrete beams were first inverted, so that the tension face was at the top, to simplify the application.
- The epoxy was hand – mixed thoroughly and applied evenly to both carbon fibre strip and the concrete surface using a roller brush.
- The CFRP strip was then smoothly hand – laid to achieve wrinkle – free surface, and the extra epoxy was squeezed out and removed keeping the thickness of epoxy between 2 – 3 mm.

The specimens were cured at room temperatures for at least two weeks before testing.

3.3.2.2.1 Beam CB1 and CF1

Beams CB1 and CF1 were served as control beams without strengthening with CFRP plates. Beam CB was made of normal concrete with a compressive strength of 66 MPa and kept as a control for the other normal concrete beams those strengthened with different CFRP plate lengths. All normal concrete beams had a concrete compressive strength of 66 MPa. Beam CF1 was made of concrete incorporating fly ash with 30% by weight of cementitious material and the compressive strength was 69 MPa. The 30% fly ash was chosen for all fly ash beams for two reasons:

1. To examine the behaviour of reinforced concrete beams made of fly ash when strengthened with CFRP system and the 20% fly ash is well known but when the 30% is used it will ensure the use of high volume of fly ash, so that the cement content can be reduced and consequently the cost and the environmental saving.

2. Because its concrete compressive strength is almost similar to the normal concrete, to simplify the comparison.

The beam CF1 was kept as a control for the other fly ash beams those strengthened with CFRP system.

3.3.2.2.2 Beam CB2 and CF2

Beam CB2 was made of normal concrete and it was strengthened with a CFRP plate of a length of 1333 mm (67% of the span length) this length was chosen because it represents the region of the pure bending, beam CB2 was also considered a control beam for beam CF2 for the comparison of the behaviour of normal and fly ash concrete beams strengthened with the same amount of CFRP. Beam CF2 was made of fly ash concrete and it was strengthened with CFRP plate of 1333 mm same as beam CB2. The external reinforcement of these two beams is shown in Figure 2. The areas covered by the CFRP plate for the shear reinforcement and for the bending moment are shown in Figure 3.

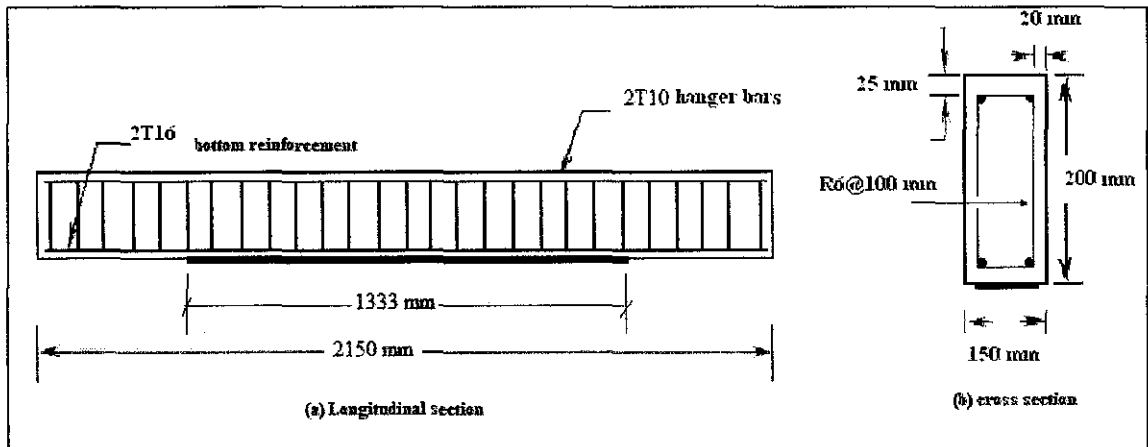


Figure 2 : External Reinforcement for CB2 and CF2

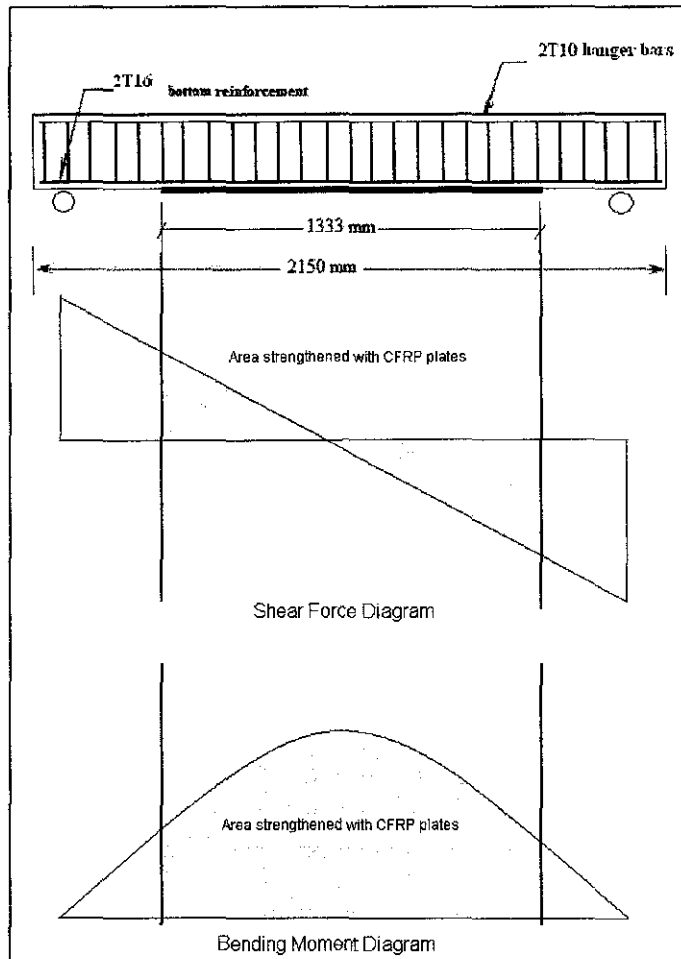


Figure 3 : Area Covered by CFRP Plate for 67% of the length

3.3.2.2.3 Beam CB3 and CF3

Beam CB3 was made of normal concrete and strengthened with a CFRP plate of length of 1667 mm (83% of the span length) which is the average length of 1333 mm and the full span length, (2000 mm). CB3 was also kept as a control for beam CF3. Beam CF3 was made of fly ash concrete and strengthened with a CFRP plate of length 1667 mm as well. The external reinforcement of CB3 and CF3 is shown in Figure 4 and the areas covered by the CFRP plate are shown in Figure 5.

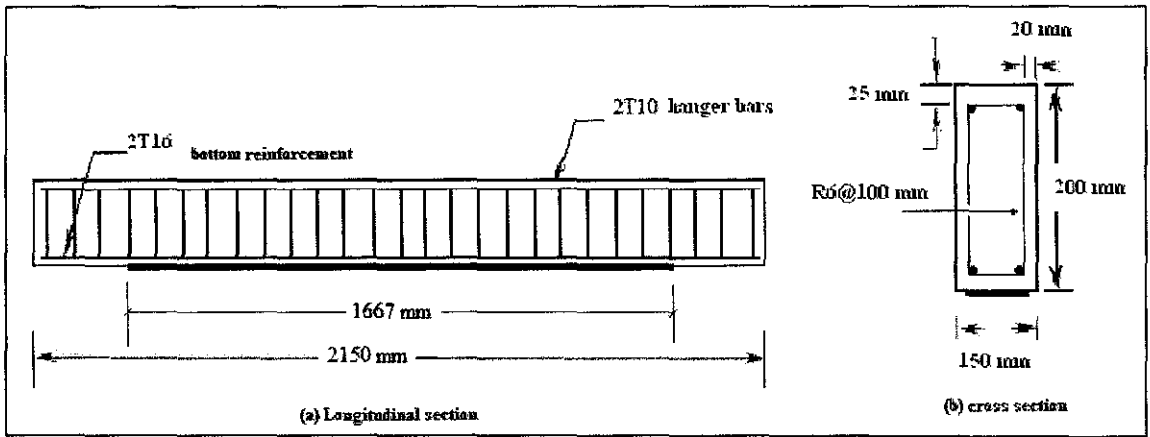


Figure 4 : External Reinforcement for CB3 and CB4

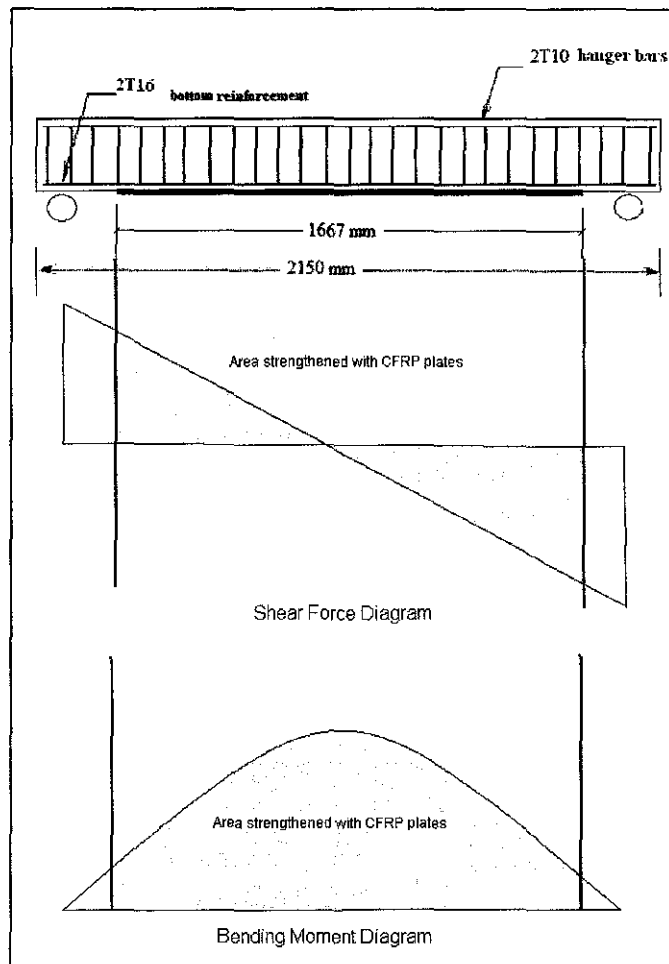


Figure 5 : Area Covered by CFRP Plate for 83% of the length

3.3.2.2.4 Beam CB4 and CF4

Beam CB4 was made of normal concrete; it was strengthened with a CFRP plate of length 2000 mm corresponding to the full span length. CB4 was also kept as a control for CF4. Beam CF4 was made of fly ash concrete and it was strengthened with a CFRP plate of a length of 2000 mm as well. The external reinforcement of CB4 and CF4 is shown in Figure 6 and the CFRP covered shown in Figure 7.

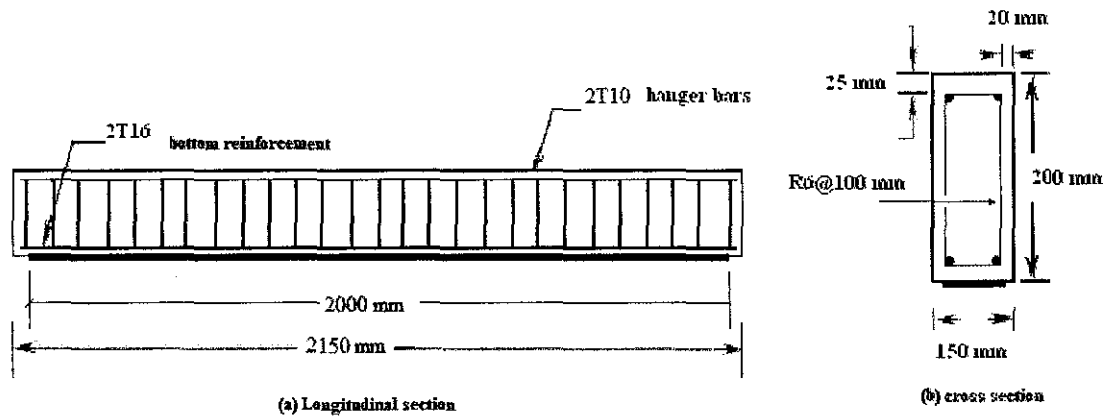


Figure 6 : External Reinforcement for CB4 and CF4

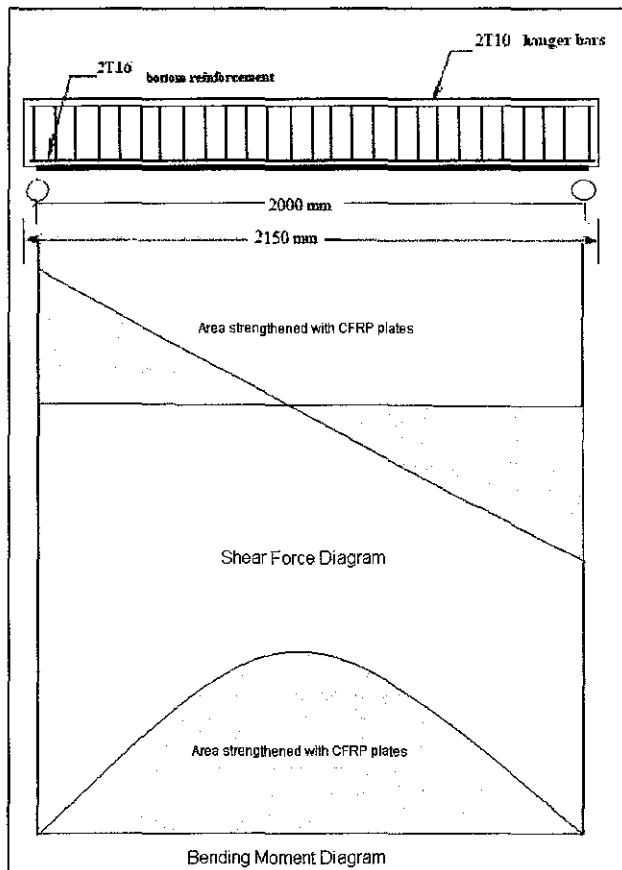


Figure 7 : Area Covered by CFRP plate for 100% length

3.3.3 Instrumentation

The constructed beams were instrumented with Linear Variable Displacement Transducer. An LVDT placed underneath the mid-span of the beams, was used to record the deflection at the mid-span point. The deflection readings were recorded every 5 seconds. Figure 8 shows the LVDT position.

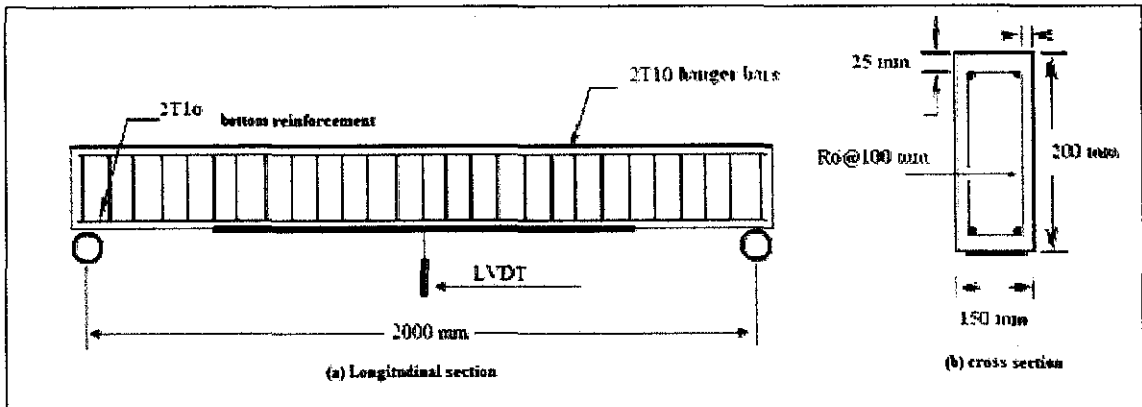


Figure 8 : Beam Instrumentation

3.4 Testing Procedure

A mid-span point load was performed on all eight test beams. The test set-up is illustrated in Figure 7. The beam were subjected to a static point loading using a hydraulic actuator with 500 kN capacity at the mid-span of the beam. The loading rate was 0.2 kN/s.

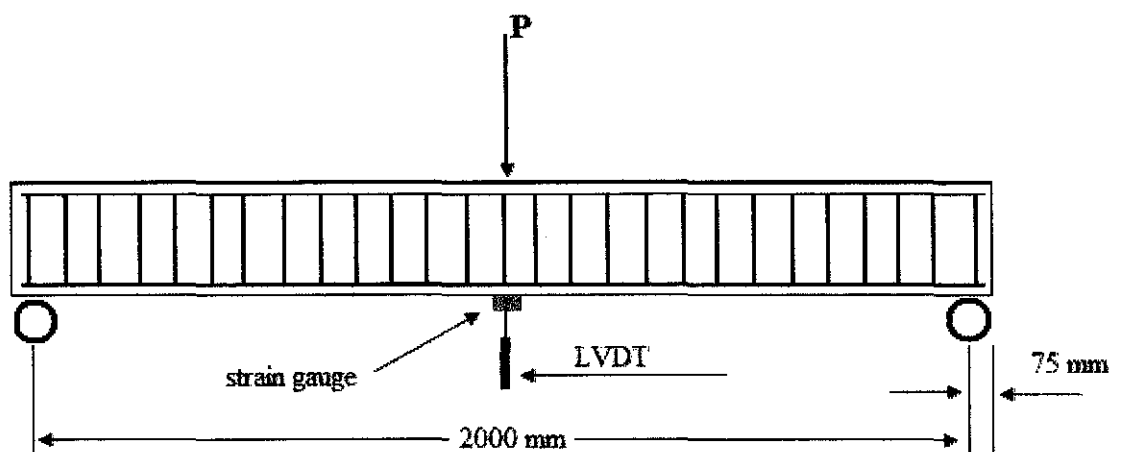


Figure 9 : Test Setup

CHAPTER 4

RESULT AND DISCUSSION

The variable for investigating the flexural behavior of high strength concrete beams strengthened with CFRP plates was the length of the CFRP plate. Beams were tested until failure occurred when subjected to central point load. During testing of beams, failure behaviour and crack pattern were observed, whereas load – deflection characteristics, ultimate and elastic load capacity and coefficient of ductility were recorded. This section presents the discussion on the results.

4.1 Modes of Failure, Crack Pattern and Failure Load

All the strengthened beams exhibited higher load carrying capacity compared to unstrengthened control beams. The ultimate failure loads for all the beams are shown below in Figure 10. Please refer to Appendix 4.1 for theoretical calculation of all the beams.

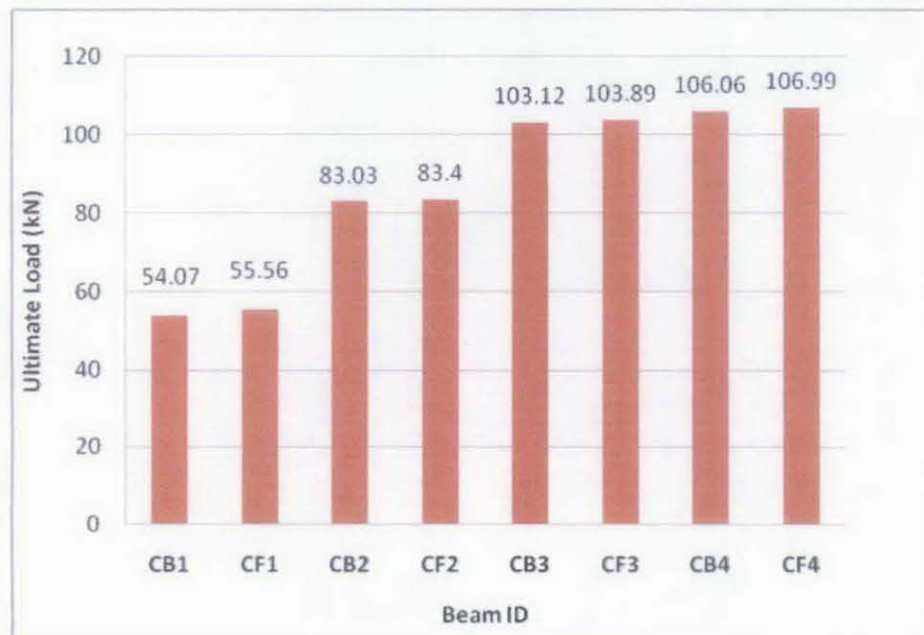


Figure 10 : Ultimate Failure Loads for The Tested Beams

Failure mode and crack pattern were physically observed during flexural testing for all the beams. Cracks were marked for their extent and configuration and numbered

according to the sequence of their appearance. The schematic drawing of the cracks and picture are shown in Figure 11 to Figure 18.

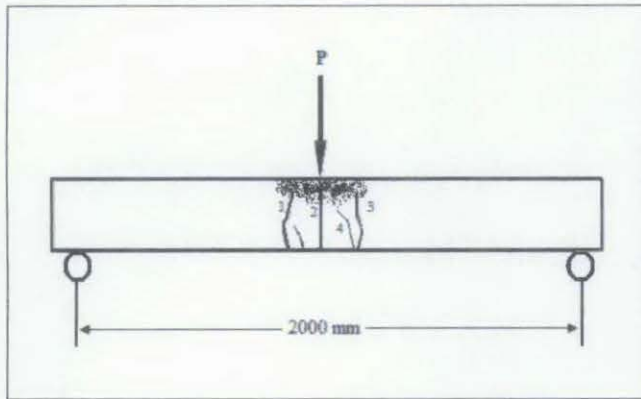


Figure 11 : Schematic Drawing and Picture of CB1 Crack Patterns

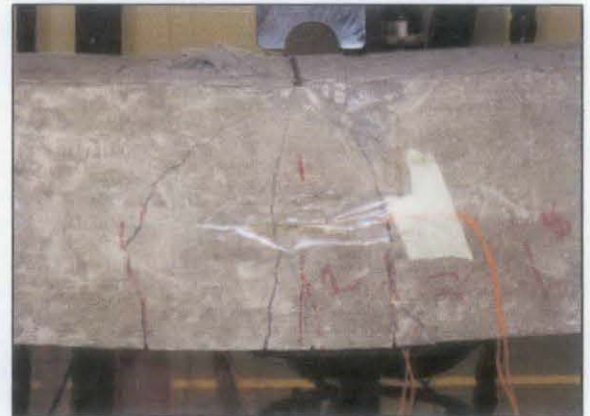
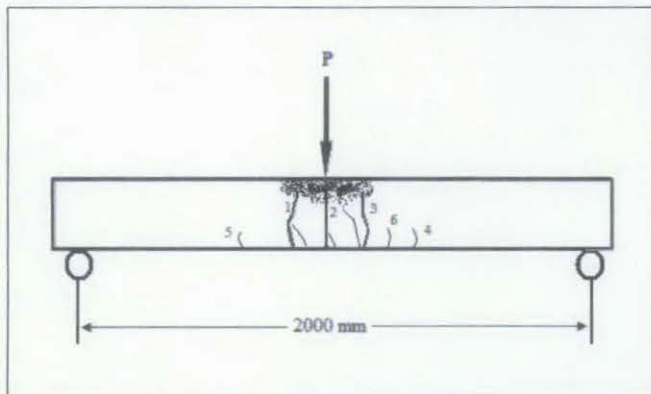


Figure 12 : Schematic Drawing and Picture of CF1 Crack Patterns

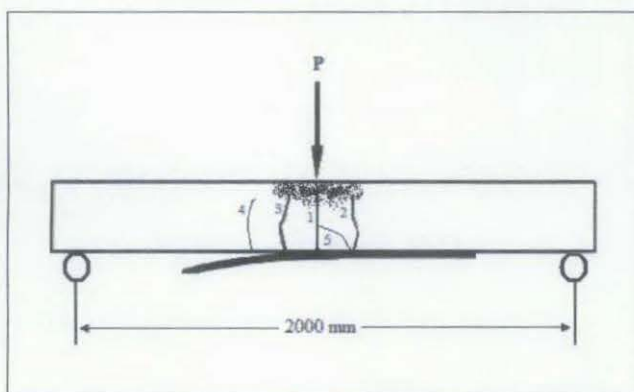


Figure 13 : Schematic Drawing and Picture of CB2 Crack Patterns

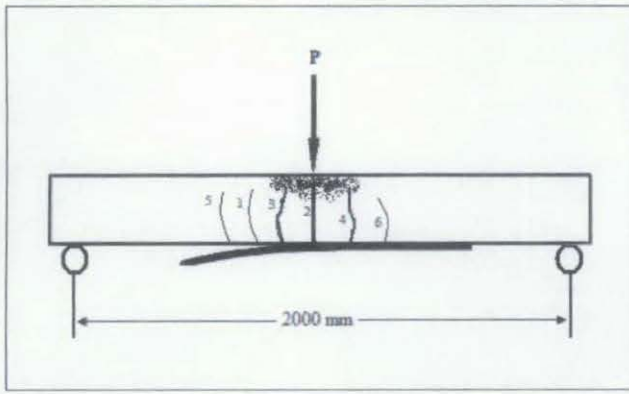


Figure 14 : Schematic Drawing and Picture of CF2 Crack Patterns

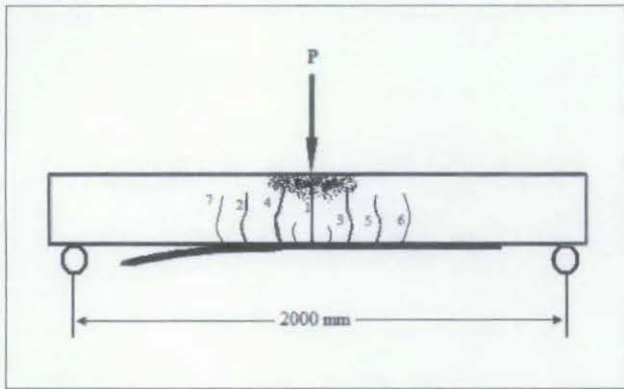


Figure 15 : Schematic Drawing and Picture of CB3 Crack Patterns

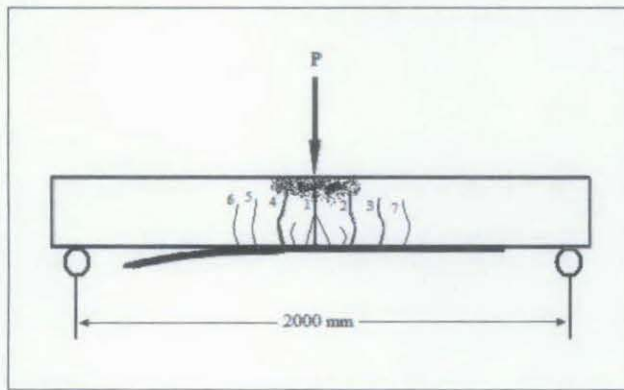


Figure 16 : Schematic Drawing and Picture of CF3 Crack Patterns

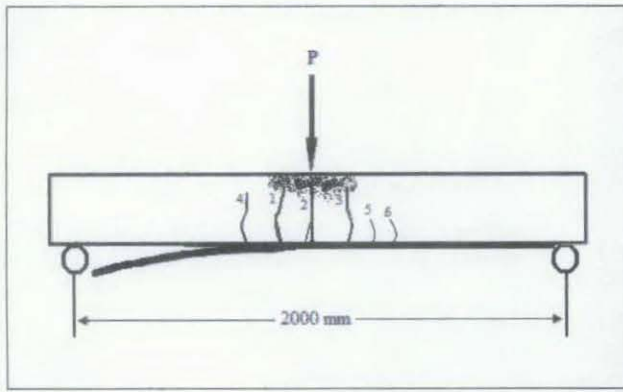


Figure 17 : Schematic Drawing and Picture of CB4 Crack Patterns

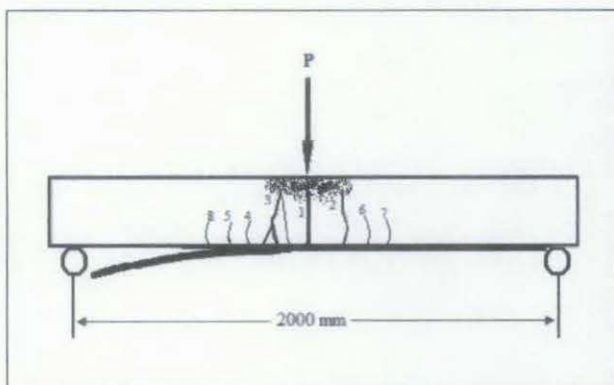


Figure 18 : Schematic Drawing and Picture of CF4 Crack Patterns

4.2 Effects of CFRP length

It can be noticed that as the amount of CFRP strengthening material increased i.e. the length of the strengthening plate the failure load will increase results in high stiffness for the strengthened member. All the strengthened beams failed in flexure with plate-end debonding, the debonding failure can be attributed to the fact that: due to the flexural cracks formed in the constant moment region as the load increased the bond between the CFRP plate and concrete started to fracture at a certain load level and the failure propagated towards the shear span until most parts of CFRP plate detached from the concrete beam. It can be seen that the bond between the CFRP plate and the concrete beam was not strong enough to ensure the rupture of the CFRP plate. There were fewer but widely spaced cracks in the non-strengthened control specimens CB1 and CF1 however; there were more but narrower cracks at relative close spacing in the strengthened beams this shows the enhanced concrete confinement due to the CFRP strengthening.

4.3 Load – Deflection Behaviour

The service load was taken at a level at which the deflection of the control beams was measured at about 35% of their ultimate loads, according to Tarek H. Almusallam and Yousef A. AL-Salloum, (2001), this means that the service loads for the control, CB1 and CF1 were about 19 KN and 19.4 KN respectively, and the corresponding deflections at that level were about 3.06 mm and 2.91 mm respectively. Therefore, all values for service loads for all strengthened beams were taken at reference deflections of 3.06 mm, for CB – series and 2.91 mm, for CF–series.

All the strengthened beams experienced mid-span deflections smaller than those of the control specimens at their failure loads. The values of the maximum deflections decrease as the stiffness of the beam increases due to the increase in the amount of strengthening material. Figures 19 and 20 shows the load–mid-span deflection relationship of the CB-series and CF-series respectively. Before the flexural cracks start, the curves are close to each other. After yielding of reinforcement bars, the strength and stiffness of the strengthened specimens were larger when compared to the control specimens. After the failure, the load–deflection curve of the strengthened beams dropped down; this behaviour was expected due to the increase in the beam stiffness as a result of increasing the length of CFRP plates.

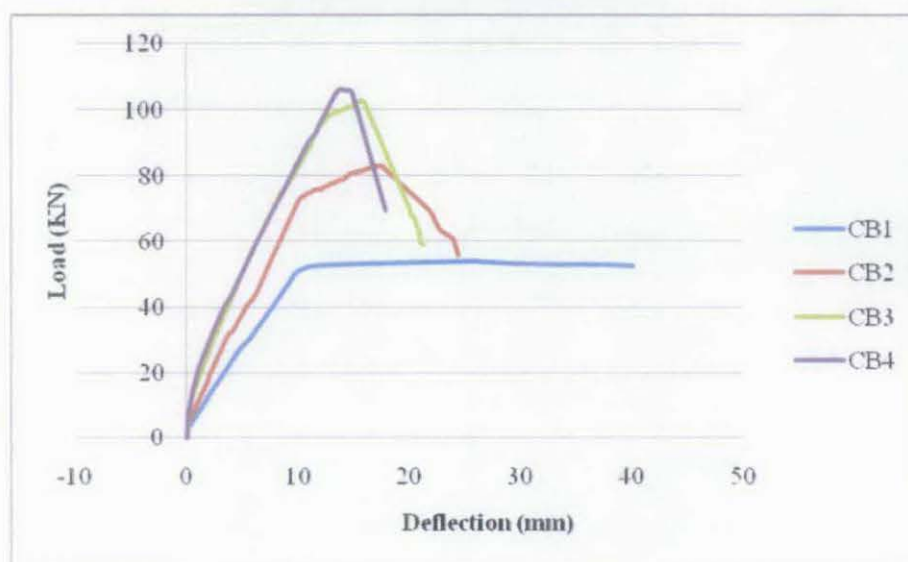


Figure 19 : Load – Deflection Relationship For The CB- Series

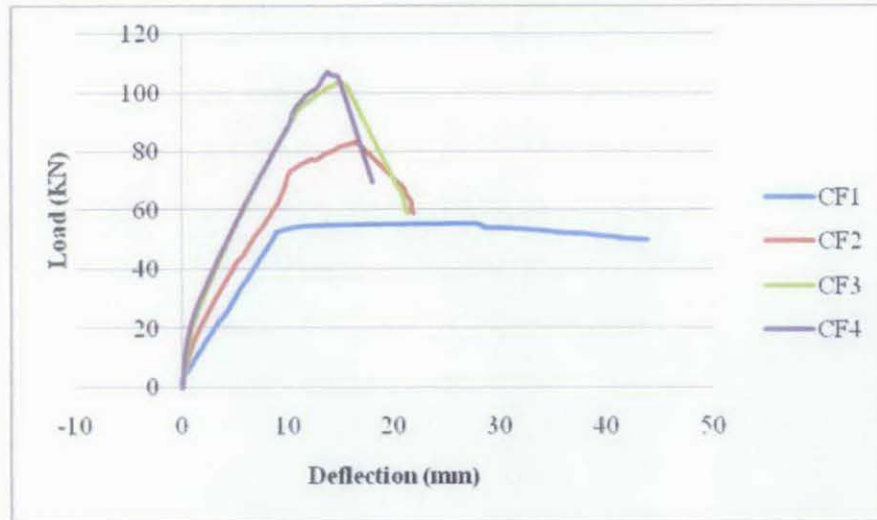


Figure 20 : Load – Deflection Relationship For The CF- Series

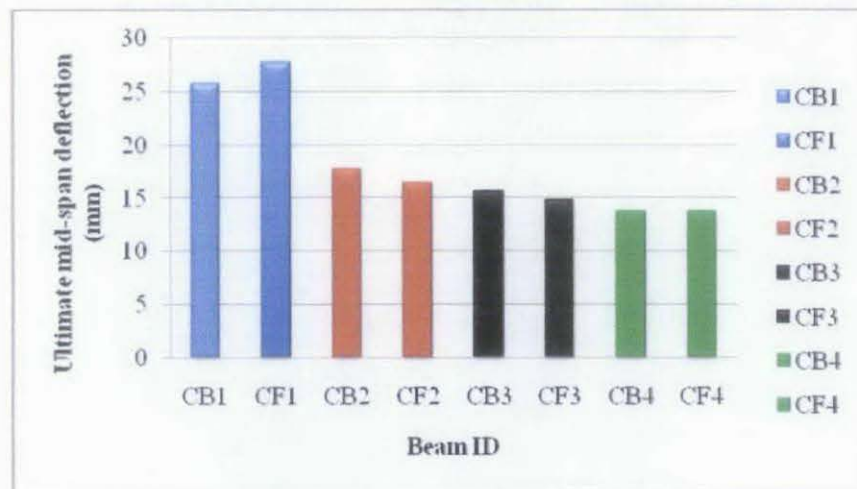


Figure 21 : Ultimate Mid – Span Deflection For All Tested Beams

4.4 CB-Series

Beam CB1 was not strengthened with CFRP plate made of normal concrete and was kept as the control specimen for CB-series. The beam exhibited small cracks at and around the loaded point and failed in flexure by crushing of concrete in compression zone; the cracks started at the tension sides and increased in width and length with the applied load. The failure load for CB1 was 54.07 KN. Beams CB2, CB3 and CB4 were strengthened with 67%, 83% and 100%, respectively, of the full span length and failed in flexure failure and plate–end debonding. The failure loads for CB2, CB3 and CB4 was 83.03 kN, 103.12kN and 106.06kN respectively which represent 53.6%,

90.7% and 96% higher than their control beam (CB1). Results for CB – Series are tabulated in Table 7.

Table 7 : Experimental Results at Service and Ultimate Loads For CB - Series

Beam ID	Service load (KN)	% gain	Ultimate load (KN)	% gain
CB1	19.0	--	54.07	--
CB2	27	42	83.03	53.6
CB3	36.0	89.5	103.12	90.7
CB4	38.0	100	106.06	96

4.5 CF-Series

Beams CF1 was kept as the control specimen for the CF-series and was made of 30% fly ash content. Beams CF1 failed in a similar manner to CB1 i.e. in flexure by concrete crushing at the compression face with ultimate failure load of 55.56 KN. Beams CF2, CF3 and CF4 were strengthened with 67%, 83% and 100%, respectively, of the full span length and they were failed in the same behaviour (flexural failure and plate-end debonding) as their respective control specimens (normal concrete) CB2, CB3 and CB4 respectively. The failure loads for CF2, CF3 and CF4 were 83.4 KN, 103.89 KN and 106.99 KN which represents 50%, 87% and 92.6% higher than their control CF1. Table 8 summarizes the loads carried by the tested beams for the CF – Series.

Table 8 : Experimental Results at Service and Ultimate Loads For CF - Series

Beam ID	Service load (KN)	% gain	Ultimate load (KN)	% gain
CF1	19.4	--	55.56	--
CF2	28.76	48	83.40	50
CF3	38.9	100.5	103.89	87
CF4	40.95	111	106.99	92.6

4.6 Ductility

Ductility usually calculated as the ratio of curvature, deflection or rotation at ultimate to yielding of steel [Tarek H. Almusallam and Yousef A. AL-Salloum, (2001)]. The ductility index in this study is obtained based on the ultimate deflection obtained from the test and the calculation of the yield deflection, and it is defined as the mid – span deflection, at ultimate load divided by the mid – span deflection at the point where the steel starts yielding. As it can be seen from load-deflection curves in Figure 19 and 20, it can be seen that all CFRP-strengthened beams performed significantly better than the control beams with respect to load-carrying capacity. However, the observed increase in the strength was associated with the reduction in the deflection capacity of the respective beams.

The ductility indices for all tested beams are shown in Table 9. The values of the ductility indices for the CFRP-strengthened beams were ranged from 2.7 – 3.5. The strengthened beams exhibited lower values as compared with the control specimens CB1 and CF1 of 4.6 and 5.0 ductility indices. The low ductility of strengthened beams indicates that the addition of the CFRP strengthening system reduces the deforming ability at the ultimate stage of loading. The reduction in ductility for the strengthened beams in reference to the control specimens is not considered to be significant. Therefore, all the strengthened beams were shown to have adequate ductility, which ensured that their failure mode was of a ductile nature.

$$\mu_D = \left(\frac{\Delta u}{\Delta y} \right)$$

Where:

μ_D : Ductility index

Δu : Mid–span deflection at ultimate load (mm), and

Δy : Mid–span deflection at yield load (mm).

Table 9 : Ultimate Deflection and Ductility Index of the Tested Beams

Beam ID	Yield deflection (mm) ^a	Ultimate deflection (mm) ^b	Ductility index $\left(\frac{\Delta_u}{\Delta_y}\right)$
CB1	5.6	25.76	4.6
CF1	5.5	27.77	5.0
CB2	5.04	17.68	3.5
CF2	5.0	16.38	3.3
CB3	5.04	15.66	3.1
CF3	5.0	14.82	3.0
CB4	5.04	13.775	2.7
CF4	5.0	13.755	2.8

a: calculated

b: experimental

CHAPTER 5

CONCLUSION

The results have shown that 1667 mm length which represented 83% of the span length was the optimum length of the CFRP plate that achieved the highest strength and beyond which the increase in the strength can be neglected. This length also achieved an adequate average ductility index, 2.65 when compared to the control sample's one which was 4.75; this yield a ductility ratio of 0.56 which can be considered an adequate ductility compared to the previous studies. The behaviour of RC beams made of concrete incorporated 30% fly ash and those made of normal concrete when strengthened with CFRP plates was similar at the first crack and ultimate levels.

REFERENCES

Ali Chahrour and Khaled Soudki. Flexural Response of reinforced concrete beams strengthened with End-Anchored partially bonded carbon fibre – reinforced polymer strips. *Journal of composites for construction*, 9, (2005), 170-177.

Bisby, L.A, Introduction to FRP Strengthening of Concrete Structure. ISIS Educational Module 4, February 2004.

Bo Gao, Jang – Kyo Kim, Christopher K. Y. Leung. Experimental study on RC beams with FRP strips bonded with rubber modified resins. *Composites Science and Technology*, 64, (2004), 2557 – 2564.

British Standards Institution, structural use of concrete: Code of practice for design and construction. BS 8110, Part 1. BSI, UK, (2002)

Esfahani M. R., M. R. Kianoush and A. R. Tajari. Flexural behaviour of reinforced concrete beams strengthened by CFRP sheets. *Engineering structures*, 29, (2007), 2428 – 2444.

Head K. H., MA (Cantab), C. Eng, FICE, FGS. Manual of Soil Laboratory Testing (Volume 1 : Soil Classification and Compaction Test)

Hollaway L C and M B Leeming. Strengthening of reinforced concrete structures using externally – bonded FRP composites in structural and civil engineering. Woodhead publishing limited, (1999)

Omrane Benjeddou, Mongi Ben Ouezdou, Aouicha Bedday. Damaged RC beams repaired by bonding of CFRP laminates. *Construction and building materials*, 21, (2007), 1301 – 1310.

Shahawy M. A., M. Arockiasamy, T. Beitelman, R. Sowrirajan. Reinforced concrete rectangular beams strengthened with CFRP laminates. *Composites part B*, 27, (1996), 225 – 233.

Tarek H. Almusallam and Yousef A. AL-Salloum. Ultimate strength prediction for RC beams externally strengthened by composite materials. *Composites Part B*: 32, (2001), 609-619.

Tarek H. Almusallam, Yousef A. Al-Salloum, Saleh H. Alsayed. Flexural Behaviour of RC Beams with Epoxy Bonded GFRP Sheets. 2nd World Engineering Congress, Sarawak, Malaysia, (2002).

Tom Norris, Hamid Saadatmanesh, and Mohammad R, Ehsani. Shear and Flexural Strengthening of R/C Beams with Carbon Fibre Sheets. *Journal of Structural Engineering*, 123, (1997), 903-911.

Toutanji H., L. Zhao and Y. Zhang. Flexural behaviour of reinforced concrete beams externally strengthened with CFRP sheets bonded with an inorganic matrix. *Engineering Structures*, 28, (2006), 557-566.

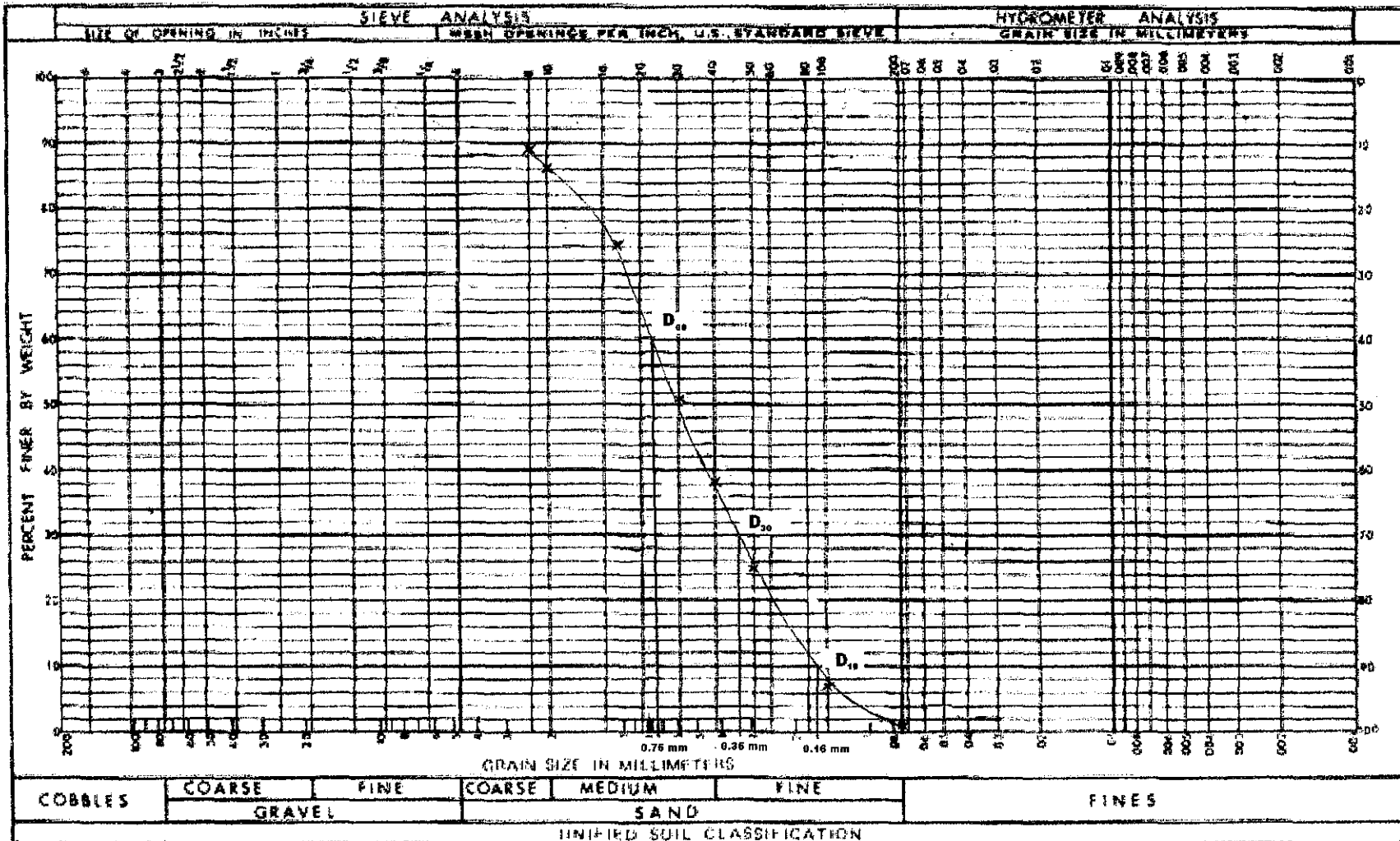
Waleed A. Thanoon, M.S. Jaafar, M. Razali A. Kadir, J. Noorzaei. Repair and structural performance of initially cracked reinforced concrete slabs. *Construction and Building Materials* 19, (2005), 595 – 603.

.

.

APPENDIX 3.1

PARTICLE SIZE DISTRIBUTION CURVE FOR COARSE AGGREGATE



Analysis

For Fine Aggregate:

D_{10} = Effective size, particle size which 10% of particles are finer, and 90% are coarser.

$$= 0.16 \text{ mm}$$

D_{30} = particle size which 30% of particles are finer, and 70% are coarser

$$= 0.35 \text{ mm}$$

D_{60} = particle size which 60% of particles are finer, and 40% are coarser

$$= 0.75 \text{ mm}$$

Uniformity coefficient (C_u) is the ratio of the 60% particle size to the 10% particle size. It is a measure of the slope of the line joining these two points in the graph shown earlier.

$$C_u = \frac{D_{60}}{D_{10}} = \frac{0.75 \text{ mm}}{0.16 \text{ mm}} = 4.6875$$

Coefficient of gradation (C_z)

$$C_z = \frac{D_{30}^2}{D_{60} \times D_{10}} = \frac{0.35^2}{0.75 \times 0.16} = 1.021$$

From BS 1377:-

For sand

$C_u \leq 6$ and $1 \leq C_z \leq 3$ (a well – graded aggregate)

$C_z < 0.1$ (a possible gap graded aggregate)

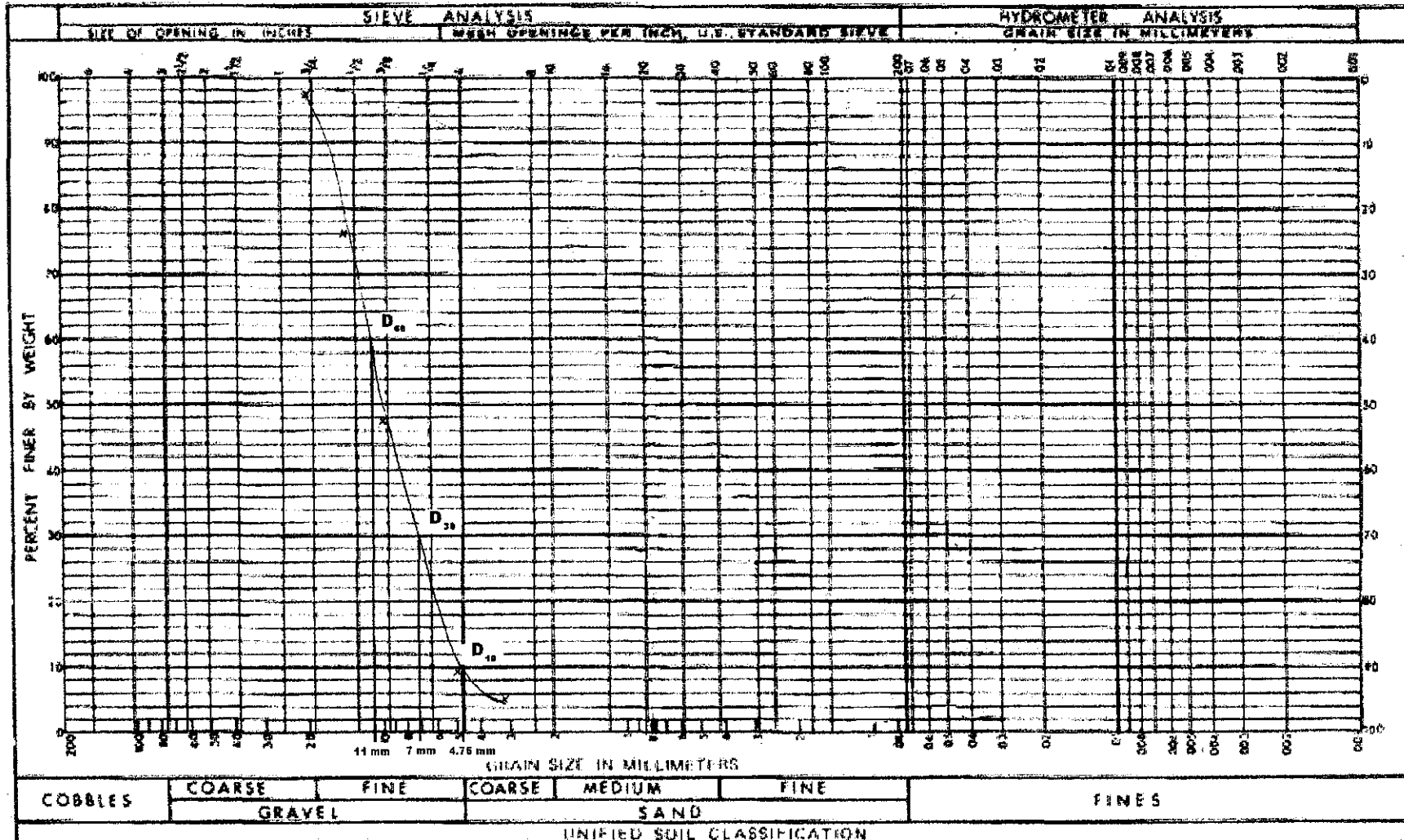
For the fine aggregate used : $C_u = 4.6875 < 6$

$$C_z = 1.021 \quad 1 \leq 1.021 \leq 3$$

And from the curve, it can be seen that it is a well graded fine aggregate.

APPENDIX 3.2

PARTICLE SIZE DISTRIBUTION CURVE FOR COARSE AGGREGATE



Analysis

For Coarse Aggregate:

D_{10} = Effective size, particle size which 10% of particles are finer, and 90% are coarser.

$$= 4.75 \text{ mm}$$

D_{30} = particle size which 30% of particles are finer, and 70% are coarser

$$= 7.00 \text{ mm}$$

D_{60} = particle size which 60% of particles are finer, and 40% are coarser

$$= 11.00 \text{ mm}$$

Uniformity coefficient (C_u) is the ratio of the 60% particle size to the 10% particle size. It is a measure of the slope of the line joining these two points in the graph shown earlier.

$$C_u = \frac{D_{60}}{D_{10}} = \frac{11\text{mm}}{4.75\text{mm}} = 2.316$$

Coefficient of gradation (C_z)

$$C_z = \frac{D_{30}^2}{D_{60} \times D_{10}} = \frac{7.00^2}{11.00 \times 4.75} = 0.94$$

From BS 1377:-

For gravel

$C_u \geq 4$ and $1 \leq C_z \leq 3$ (a well – graded aggregate)

$C_z < 0.1$ (a possible gap graded aggregate)

For the coarse aggregate used : $C_u = 2.316 < 4$

$$C_z = 0.94 \quad 0.94 < 1$$

From the particle size distribution curve, it can be seen that the slope between D_{60} and D_{10} is slightly steep. Thus, the result is slightly poor sorted coarse aggregate.

APPENDIX 3.3

DESIGN OF CFRP

Using ISIS Education Module 4

ISIS Canada, L.A Bisby, Queen's University, 2004

Concrete compressive strength, $f_{cu} = 50$ MPa

Area of steel, $A_s = 402$ mm²

Steel yield strength, $f_y = 460$ MPa

Steel modulus of elasticity, $E_s = 230$ GPa

FRP modulus of elasticity $E_{frp} = 155$ GPa

Area of FRP, $A_{frp} = 120$ mm²

$\epsilon_{frpu} = 1.55\%$

$\Phi_{frp} = 0.75$ (ISISCanada)

$$Cc = Ts + T_{frp}$$

$$Cc = 0.45 f_{cu} b * 0.9x$$

$$Ts = 0.95 f_y A_s$$

$$T_{frp} = 0.75 E_{frp} A_{frp} \epsilon_{frp}$$

$$0.405 f_{cu} bx = 0.95 f_y A_s + 0.75 E_{frp} A_{frp} \epsilon_{frp}$$

$$0.405 * 50 * 150 * x = 0.95 * 460 * 402 + 0.75 * 155000 * 120 * \left(0.0035 * \left(\frac{200 - x}{x} \right) \right)$$

$$x^2 - 41.8x - 3214.8 = 0$$

$$x = \frac{-b \pm \sqrt{b^2 - 4ac}}{2a}$$

$$x = 81.4mm$$

Calculate the strain in the FRP, ϵ_{frp}

$$\varepsilon_{frp} = \varepsilon_{cu} * \left(\frac{h-x}{x} \right)$$

$$\varepsilon_{frp} = 0.0051 < \varepsilon_{frpu} = 0.0155$$

$$\varepsilon_s = \varepsilon_{cu} * \left(\frac{d-x}{x} \right)$$

$$\varepsilon_s = 0.0034 > \varepsilon_y = 0.002$$

The steel has yielded thus the amount of FRP is appropriate

The factored moment resistance:

$$M = 0.95 f_y A_s (d - 0.45x) + 0.75 E_{frp} A_{frp} \varepsilon_{frp} (h - 0.45x)$$

$$M = 33.3 \text{ KN.m}$$

The factored moment of unstrengthened beam = 23.5 KN.m

Thus the FRP has increased the flexural strength of the beam by about 42%.

APPENDIX 3.4

BEAM DESIGN AND ANALYSIS

Using BS 8110

Assume:

Live load = 3.0 KN/m^2

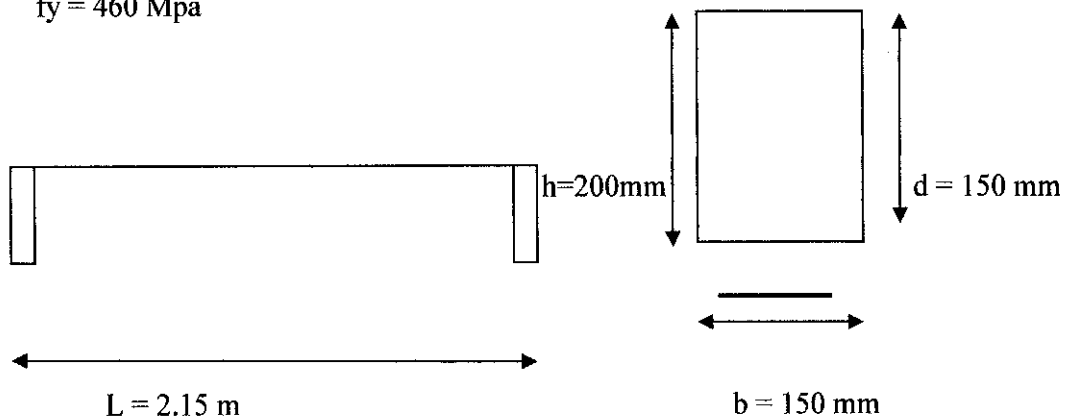
Finishing load = 1.0 KN/m^2

Thickness of slab = 150 mm

Unit weight of concrete = 24.0 KN/m^3

$f_{cu} = 50 \text{ Mpa}$

$f_y = 460 \text{ Mpa}$



Loading:

Slab dead load (g_k) = self-weight + finishes

$$= 0.15 * 24 + 1.0$$

$$= 4.6 \text{ KN/m}^2$$

Slab imposed load (q_k) = 3.0 KN/m^2

Slab ultimate load = $1.4g_k + 1.6q_k$

$$= 1.4 * 4.6 + 1.6 * 3$$

$$= 11.24 \text{ KN/m}^2$$

Beam dead load = self-weight

$$= 0.15 * 0.2 * 24 = 0.72 \text{ KN/m}$$

$$\begin{aligned}\text{Beam ultimate load} &= 1.4gk \\ &= 1.4 \times 0.72 \\ &= 1.01 \text{ KN/m}\end{aligned}$$

Design load:

Assume the slab is simply supported; beam 1-2 supports a uniformly distributed load from a 1.8 m width of slab plus its self-weight.

$$\begin{aligned}\text{Design load (w) on beam 1-2} &= \text{slab load} + \text{self-weight of beam} \\ &= 11.24 \times 2.0 + 1.01 = 23.5 \text{ KN/m}\end{aligned}$$

Design moment (M):

$$M = wl^2/8 = 23.5 \times 2.0^2/8 = 11.75 \text{ KN.m}$$

Design shear force (V):

$$V = wl/2 = 23.5 \times 2.0/2 = 23.5 \text{ KN}$$

Area of steel:

$$K = M / f_{cu} b d^2 = 11.75 \times 10^6 / 50 \times 150 \times 160^2 = 0.061 < 0.156$$

Thus compression reinforcement does not required.

$$z/d = 0.5 + \sqrt{0.25 - K/0.9}$$

$$(0.95 \leq z/d \leq 0.775)$$

$$z/d = 0.93$$

$$A_s = \left(\frac{M}{0.95 f_{yz}} \right) = 180.7 \text{ mm}^2$$

$$A_{s \text{ provide}} = 402 \text{ mm}^2$$

Use 2 T 16

Shear link design:

$$V = 23.5 \text{ KN}$$

$$\frac{100 A_s}{bd} = \frac{100 \times 402}{150 \times 150} = 1.79$$

$$v_c = 0.98 N / \text{mm}^2$$

$f_{cu} > 25$

$$v_c = \left(\frac{50}{25}\right)^{\left(\frac{1}{3}\right)} * 0.98 = 1.23 N / mm^2$$

$$0.5v_c = 0.62$$

$$v = \frac{V}{bd} = \frac{23.5 * 10^3}{150 * 160} = 0.98 N / mm^2$$

$$v > 0.5v_c$$

$$v_c + 0.4 = 1.23 + 0.4 = 1.63$$

$$0.5v_c < v < v_c + 0.4$$

$$\frac{A_{sv}}{sv} = \frac{0.4 * b}{0.95 * f_{yv}} = \frac{0.4 * 150}{0.95 * 250} = 0.253$$

$$sv = 100mm$$

$$A_{sv} = 56.5mm^2$$

Provide 6m links at 100 spacing c.c

Deflection check:

$$\text{Actual span/depth ratio} = \frac{2000}{160} = 12.5$$

$$\frac{M}{bd^2} = \frac{11.75 * 10^6}{150 * 160^2} = 3.06 N / mm^2$$

$$f_s = \frac{2}{3} * f_y * \frac{A_{s_{required}}}{A_{s_{provide}}} * \frac{1}{\beta_b}$$

Where β_b is the percentage moment redistribution, equal 1.0 for simply supported beam.

$$f_s = \frac{2 * 460 * 180.7}{3 * 402} = 137.85 N / mm^2$$

$$\text{Modification factor} = 0.55 + \left[\frac{477 - f_s}{120 \left(0.9 + \frac{M}{bd^2} \right)} \right] \leq 2.0 = 1.26 < 2.0$$

The permissible span/depth ratio = $20 * 1.26 = 25.2 > \text{actual}$

Therefore the beam satisfies deflection criteria in BS 8110

APPENDIX 4.1

BEAM MAXIMUM MOMENT CALCULATION

Theoretical Calculation for CB₁

$$f_{cu} = 66 \text{ MPa}$$

$$T=C$$

$$0.95f_y A_s = 0.405f_{cu} bx$$

$$0.95 \times 460 \times 402 = 0.405 \times 66 \times 150 \times x$$

$$x = 43.8144 \text{ mm}$$

$$z = d - 0.45x$$

$$z = 161 \text{ mm} - 0.45(43.8144 \text{ m})$$

$$z = 141.28352 \text{ mm}$$

$$M=T.z$$

$$M = 0.95f_y A_s z$$

$$M = 0.95 \times 460 \times 402 \times 141.28352$$

$$M = 24.82 \text{ kN.m}$$

$$W = \frac{4M}{L} = \frac{4(24.82 \text{ kN.m})}{2 \text{ m}} = 49.64 \text{ kN}$$

Theoretical Calculation for CF₁

$$f_{cu} = 69 \text{ MPa}$$

$$T=C$$

$$0.95f_y A_s = 0.405f_{cu} bx$$

$$0.95 \times 460 \times 402 = 0.405 \times 69 \times 150 \times x$$

$$x = 41.9095 \text{ mm}$$

$$z = d - 0.45x$$

$$z = 161 \text{ mm} - 0.45(41.9095 \text{ m})$$

$$z = 142.1407 \text{ mm}$$

$$M=T.z$$

$$M = 0.95f_y A_s z$$

$$M = 0.95 \times 460 \times 402 \times 142.1407$$

$$M = 24.97 \text{ kN.m}$$

$$W = \frac{4M}{L} = \frac{4(24.97 \text{ kN.m})}{2 \text{ m}} = 49.94 \text{ kN}$$

Theoretical Calculation for CB₂, CB₃, CB₄

Using ISIS Canada

$$f_c = 66 \text{ MPa}$$

$$A_s = 402 \text{ mm}^2$$

$$f_y = 460 \text{ MPa}$$

$$E_s = 230 \text{ GPa} = 230 \times 10^3 \text{ MPa}$$

$$A_{f_{rp}} = 120 \text{ mm}^2$$

$$E_{f_{rp}} = 150 \text{ GPa} = 150 \times 10^3 \text{ MPa}$$

From the experiment, it is observed that the failure of the beam was due to crushing of the concrete due to compression, after yielding of the internal steel reinforcement.

$$\begin{aligned} \alpha_1 &= 0.85 - 0.0015f_c \gg 0.67 \\ &= 0.85 - 0.0015(66) = 0.751 > 0.67 \\ \beta_1 &= 0.97 - 0.0025f_c \gg 0.67 \\ &= 0.97 - 0.0025(66) = 0.805 > 0.67 \end{aligned}$$

$$C_c = T_s + T_{f_{rp}}$$

$$C_c = \Phi_c \alpha_1 f_c \beta_1 b c$$

$$T_s = \Phi_s A_s f_s \text{ with } f_s \ll f_y$$

$$T_{f_{rp}} = \Phi_{f_{rp}} A_{f_{rp}} E_{f_{rp}} \varepsilon_{f_{rp}} \text{ with } \varepsilon_{f_{rp}} \ll \varepsilon_{f_{rp}u}$$

$$\Phi_c \alpha_1 f_c \beta_1 b c = \Phi_s A_s f_s + \Phi_{f_{rp}} A_{f_{rp}} E_{f_{rp}} \varepsilon_{f_{rp}}$$

$$\begin{aligned} 0.6(0.751)(66)(0.805)(150)c \\ = 0.85(460)(402) + 0.75(150000)(120) \left(0.0035 \frac{200 - c}{c} \right) \end{aligned}$$

$$c = 68.84 \text{ mm}$$

$$\varepsilon_{f_{rp}} = \varepsilon_{cu} \frac{h - c}{c}$$

$$\varepsilon_{f_{rp}} = 0.0035 \left[\frac{200 - 68.84}{68.84} \right] = 0.0067$$

The CFRP used are Sika CarboDur M and the strain at failure is 1.2%

$$\therefore \varepsilon_{f_{rp}u} = 0.012$$

$$0.0067 < 0.012$$

$\varepsilon_{f_{rp}} < \varepsilon_{f_{rp}u}$ ■ failure by concrete crushing

$$\varepsilon_s = \varepsilon_{cu} \frac{d - c}{c}$$

$$\varepsilon_s = 0.0035 \left[\frac{161 - 68.84}{68.84} \right] = 0.0047$$

$\varepsilon_y = 0.002 \rightarrow$ for steel to yield

$$0.0047 > 0.002$$

$\varepsilon_s > \varepsilon_y$ ■ the steel has yielded

$$\begin{aligned}
 a &= \beta_1 c \\
 &= 0.805(68.84)
 \end{aligned}$$

To calculate the moment,

$$\begin{aligned}
 M_r &= \phi_s A_s f_s \left(d - \frac{a}{2} \right) + \phi_{f_{rp}} A_{f_{rp}} E_{f_{rp}} \epsilon_{f_{rp}} \left(h - \frac{a}{2} \right) \\
 &= 0.85(460)(402) \left(161 - \frac{0.805 \times 68.84}{2} \right) \\
 &\quad + 0.75(150000)(120)(0.0067) \left(200 - \frac{0.805 \times 68.84}{2} \right) \\
 &= 36.53 \text{ kN.m}
 \end{aligned}$$

$$\begin{aligned}
 W &= \frac{4M}{L} = \frac{4(36.53 \text{ kN.m})}{2} \\
 &= 73.06 \text{ kN}
 \end{aligned}$$

Theoretical Calculation for CF₂CF₃CF₄

Using ISIS Canada

$$f_c = 69 \text{ MPa}$$

$$A_s = 402 \text{ mm}^2$$

$$f_y = 460 \text{ MPa}$$

$$E_s = 230 \text{ GPa} = 230 \times 10^3 \text{ MPa}$$

$$A_{frp} = 120 \text{ mm}^2$$

$$E_{frp} = 150 \text{ GPa} = 150 \times 10^3 \text{ MPa}$$

From the experiment, it is observed that the failure of the beam was due to crushing of the concrete due to compression, after yielding of the internal steel reinforcement.

$$\begin{aligned} \alpha_1 &= 0.85 - 0.0015f_c \gg 0.67 \\ &= 0.85 - 0.0015(69) = 0.746 > 0.67 \\ \beta_1 &= 0.97 - 0.0025f_c \gg 0.67 \\ &= 0.97 - 0.0025(69) = 0.797 > 0.67 \end{aligned}$$

$$C_c = T_s + T_{frp}$$

$$C_c = \phi_c \alpha_1 f_c \beta_1 b c$$

$$T_s = \phi_s A_s f_s \text{ with } f_s \ll f_y$$

$$T_{frp} = \phi_{frp} A_{frp} E_{frp} \epsilon_{frp} \text{ with } \epsilon_{frp} \ll \epsilon_{frpu}$$

$$\phi_c \alpha_1 f_c \beta_1 b c = \phi_s A_s f_s + \phi_{frp} A_{frp} E_{frp} \epsilon_{frp}$$

$$0.6(0.746)(69)(0.797)(150)c$$

$$= 0.85(460)(402) + 0.75(150000)(120) \left(0.0035 \frac{200 - c}{c} \right)$$

$$c = 67.57 \text{ mm}$$

$$\epsilon_{frp} = \epsilon_{cu} \frac{h - c}{c}$$

$$\epsilon_{frp} = 0.0035 \left[\frac{200 - 67.57}{67.57} \right] = 0.0069$$

The CFRP used are Sika CarboDur M and the strain at failure is 1.2%

$$\therefore \epsilon_{frpu} = 0.012$$

$$0.0069 < 0.012$$

$\epsilon_{frp} < \epsilon_{frpu}$ ■ failure by concrete crushing

$$\varepsilon_s = \varepsilon_{cu} \frac{d - c}{c}$$

$$\varepsilon_s = 0.0035 \left[\frac{161 - 67.57}{67.57} \right] = 0.0048$$

$$\varepsilon_y = 0.002 \rightarrow \text{for steel to yield}$$

$$0.0048 > 0.002$$

$\varepsilon_s > \varepsilon_y$ ■ the steel has yielded

$$\begin{aligned} a &= \beta \cdot c \\ &= 0.797(67.57) \end{aligned}$$

To calculate the moment,

$$M_r = \phi_s A_s f_s \left(d - \frac{a}{2} \right) + \phi_{frrp} A_{frrp} E_{frrp} \varepsilon_{frrp} \left(h - \frac{a}{2} \right)$$

$$\begin{aligned} &= 0.85(460)(402) \left(161 - \frac{0.797 \times 67.57}{2} \right) \\ &\quad + 0.75(150000)(120)(0.0069) \left(200 - \frac{0.797 \times 67.57}{2} \right) \end{aligned}$$

$$= 37.17 \text{ kN.m}$$

$$\begin{aligned} W &= \frac{4M}{L} = \frac{4(37.17 \text{ kN.m})}{2} \\ &= 74.34 \text{ kN} \end{aligned}$$